nature geoscience

ARTICLES

https://doi.org/10.1038/s41561-022-00971-w

Check for updates

Twentieth-century Azores High expansion unprecedented in the past 1,200 years

Nathaniel Cresswell-Clay[1], Caroline C. Ummenhofer[1]✉, Diana L. Thatcher[2], Alan D. Wanamaker[2], Rhawn F. Denniston[3], Yemane Asmerom[4] and Victor J. Polyak[4]

The Azores High is a persistent atmospheric high-pressure ridge over the North Atlantic surrounded by anticyclonic winds that steer rain-bearing weather systems and modulate the oceanic moisture transport to Europe. The areal extent of the Azores High thereby affects precipitation across western Europe, especially during winter. Here we use observations and ensemble climate model simulations to show that winters with an extremely large Azores High are significantly more common in the industrial era (since CE 1850) than in pre-industrial times, resulting in anomalously dry conditions across the western Mediterranean, including the Iberian Peninsula. Simulations of the past millennium indicate that the industrial-era expansion of the Azores High is unprecedented throughout the past millennium (since CE 850), consistent with precipitation proxy evidence from Portugal. Azores High expansion emerges after CE 1850 and strengthens into the twentieth century, consistent with anthropogenically driven warming.

The Iberian Peninsula has distinct spatial climate variability; the southern and eastern regions are characterised by a temperate Mediterranean climate, while the northwest is exposed to Atlantic weather systems. Hot, dry summers and cool, wet winters make winter rainfall vital for the region's ecological and economic health. The region receives on average 732 mm yr^{-1} ($\pm$141 mm yr^{-1}) of rain, roughly 40% of this during winter months. Yet a robust annual drying of 5 to 10 mm yr^{-1} per decade has been recorded in the Iberian Peninsula throughout the second half of the twentieth century[1] (Fig. 1a), with a further 10–20% drop in winter precipitation expected by the end of the twenty-first century[2]. These projected changes make agriculture of the Iberian region some of the most vulnerable in Europe[3]. Olive-growing regions in southern Spain are projected to suffer a 30% decline in production by 2100[4], and grape-growing regions across the Iberian Peninsula are projected to decrease in area between 25% and 99% by 2050 due to severe water deficits that render land unsuitable for viticulture[5,6]. In this Article, we explore the changing atmospheric conditions since the onset of the industrial era that have contributed to these regional hydroclimatic changes by assessing how the characteristics of the Azores High have varied over the past 1,200 years.

The Azores High is a subtropical high-pressure system that extends over the eastern subtropical North Atlantic and western Europe during winter and is associated with anticyclonic winds in the subtropical North Atlantic[7]. It is formed by dry air aloft descending in the subtropics and coincides with the downward branch of the Hadley Circulation. The westerly winds at the southern edge of the subtropical high pick up moisture as they traverse the North Atlantic and feed winter rainfall on the Iberian Peninsula (Fig. 1). As the size and intensity of the Azores High varies, shifts in prevailing winds alter the transport of moisture onto Europe, making the Azores High an effective gatekeeper of precipitation on the continent. Indeed, variable large-scale dynamics are seen as the primary cause of evolving moisture availability in southern Europe and the Iberian Peninsula[8–10]. Trends in Iberian hydroclimate hence suggest a change in the behaviour of the Azores High. In this study, we show that the Azores High has changed dramatically in the past century and that these changes in North Atlantic climate are unprecedented within the past millennium. Diagnostic variables such as temperature have shown substantial natural variability over the past millennium;[11] we expect to see a correspondence between these variables and the Azores High. However, exploring the variability in the Azores High provides a dynamical insight that can explain many of the observed and reconstructed changes to the hydroclimate of western Europe.

Globally, substantial changes in the subtropical high-pressure systems have been documented in recent decades, yet regionally they exhibit different trends: while the high-pressure ridge in the western North Pacific is projected to undergo a robust weakening and eastward shift in the twenty-first century, the high-pressure ridges in the eastern North Pacific and the western North Atlantic are expected to intensify[12–14]. Furthermore, responses to climate change can be expected to emerge at different times depending on region and metric[15]. Zonal asymmetries in the Northern Hemisphere make it difficult to identify clear hemisphere-wide circulation trends and caution that correspondence of the subtropical atmospheric circulation to global temperature changes—while to first-order set by hemispheric temperature gradients—deviates substantially at regional scales and exhibits variability that extends beyond a hemispheric or basin-wide response to changing temperatures[16,17]. In the eastern North Atlantic, Eurasia creates a continental barrier making the Azores High a zonally distinct feature that responds to changes in continental heating over western Europe and Africa[17,18]. Its western edge, often referred to as the Bermuda High, modulates rainfall in the southeastern United States by inducing southeasterly winds that carry moisture from the Gulf of Mexico[19–21]. The northern portion of the Azores High modulates weather in Europe by interacting with the westerly winds that form the North Atlantic storm track. The storm track has important interactions with surrounding orography and the underlying ocean; changes to circulation and

[1]Department of Physical Oceanography, Woods Hole Oceanographic Institution, Woods Hole, MA, USA. [2]Department of Geological and Atmospheric Sciences, Iowa State University, Ames, IA, USA. [3]Department of Geology, Cornell College, Mount Vernon, IA, USA. [4]Department of Earth and Planetary Sciences, University of New Mexico, NM, USA. ✉e-mail: cummenhofer@whoi.edu

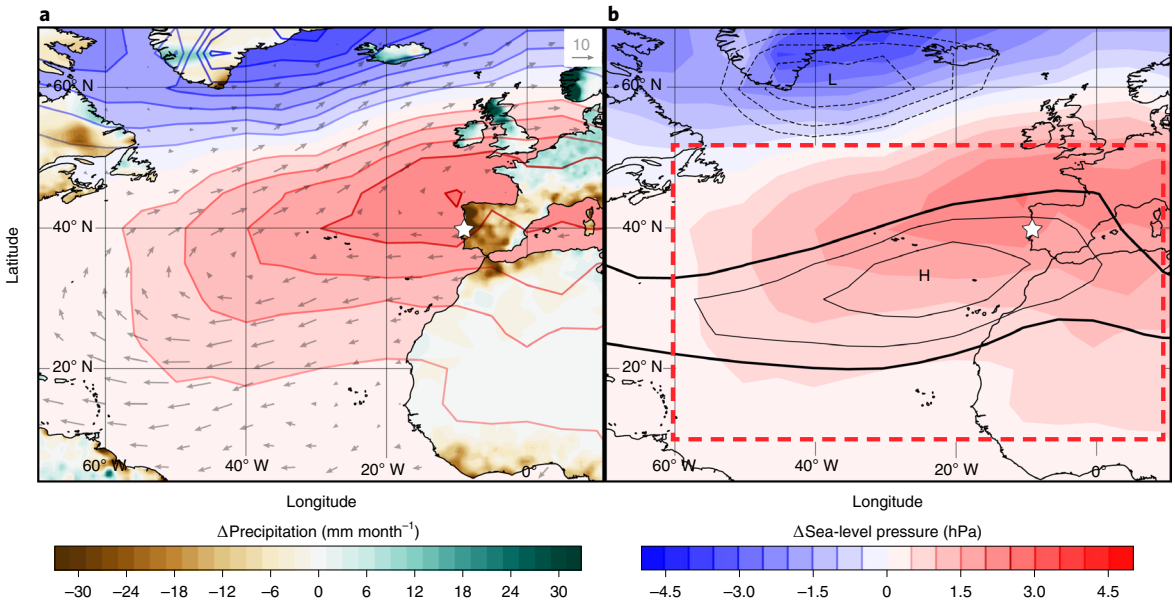

Fig. 1 | AHA and its recent expansion. a, The difference (Δ) between 1980–2007 and 1950–1979 in mean winter sea-level pressure in hPa (blue–red contours, calculated using HadSLP2 observations), terrestrial precipitation mm month^{-1} (brown–green contours, calculated using GPCC precipitation) and moisture transport in g kg^{-1} m s^{-1} (grey arrows). **b**, The difference in mean winter sea-level pressure between 1980–2007 and 1950–1979 (blue–red contours) as well as the region considered when calculating AHA (red dashed box) and the winter sea-level pressure climatology in this region (black contours: low-pressure contours are dashed; high pressures are solid). The centre of the Azores High is indicated with an 'H' while the centre of the corresponding Icelandic Low is indicated with an 'L'; the star above central Portugal indicates the location of the Buraca Gloriosa cave.

temperature in the ocean mechanistically affect its heat and moisture flux with the atmosphere[22–24]. As the oceans and atmosphere have changed in recent decades, there has been a poleward shift in the North Atlantic storm track, along with an increase in anticyclone frequency at the poleward edge of the Azores High[25,26].

Changes in the North Atlantic storm track are linked to the variability of the North Atlantic Oscillation (NAO), an atmospheric dipole representing the difference in sea-level pressure (SLP) between the Azores High and the Icelandic Low[27]. During a positive (negative) NAO phase, there is an enhanced (reduced) pressure difference between the Azores High and Icelandic Low. Climate reconstructions suggest that the NAO has experienced multidecadal variability in the late Holocene, with prolonged positive or negative phases[28–33], although differences exist in these estimates[33]. A positive NAO phase has dominated since the 1980s[34]. Here we analyse North Atlantic atmospheric variability with a subtropical perspective by focusing on the Azores High independently of the Icelandic Low. The subtropical perspective provides a direct understanding of regional climate variability in the western Mediterranean, reveals dramatic changes to North Atlantic climate throughout the past century and can provide insight into the impact of future warming on the dynamics of the Azores High and associated hydroclimate.

Expansion of the Azores High in the twentieth century

In this study, we explore changes in the size and intensity of the Azores High over the past millennium. The Azores High also exhibits substantial low-frequency variability in its location and shape; however, recent trends are most clearly captured by analysing its size. To quantify this aspect of variability, we introduce an Azores High area (AHA) diagnostic. The AHA is defined as the area over the North Atlantic sector that had a mean winter (December–January–February) SLP greater than 0.5 standard deviations from the spatio-temporal SLP long-term mean. This relative threshold captures the spatial distribution of anticyclonic winds in the North Atlantic (Fig. 1 and Methods). By setting a high-pressure threshold and measuring the region in which the SLP is higher than this threshold, the AHA combines a measure of intensity and size to diagnose Azores High variability. The region considered when calculating the AHA is bounded by the 60° W and 10° E meridians as well as the 10° N and 52° N latitudes and includes much of the North Atlantic and western Europe (Fig. 1). The inclusion of western Europe in this region allows the diagnostic to capture the tendency of the Azores High to encroach over continental Europe during the winter months.

To explore variability and trends in the Azores High, we make use of observations, reanalysis products and an ensemble of state-of-the-art climate model simulations of the past 1,200 years (Methods). We use the Last Millennium Ensemble[35] (LME), which is an ensemble of numerical simulations that model the climate of the past millennium using the Community Earth System Model version 1 (CESM1.1). The ensemble contains an experiment with 13 member simulations that receive identical transient forcing, consisting of well-mixed atmospheric greenhouse gases (GHGs), volcanic, ozone/aerosols, solar, and orbital forcing, among others, over the period CE 850 to CE 2005.

The AHA metric is calculated using SLP from observations, reanalysis products and climate model simulations (Fig. 2 and Extended Data Table 1). The time evolution of the AHA over the period 1850–2005 reveals considerable year-to-year variability, which is well captured among the three different observational and reanalysis products, as well as the LME (Fig. 2a,b). Furthermore, we identified winters in which the Azores High had an extremely large region above the high-pressure threshold (within the largest 10% of winter AHA). During these extreme winters, the high-pressure ridge over the North Atlantic and Europe is 52.7% (roughly 6 million km^2) larger than during non-extreme winters. In the period common to all data products (1900–2005), 10 of the 12 extreme Azores High winters identified in observations were also extreme in the reanalysis data. This indicates close agreement among the observational and reanalysis data (Fig. 2a).

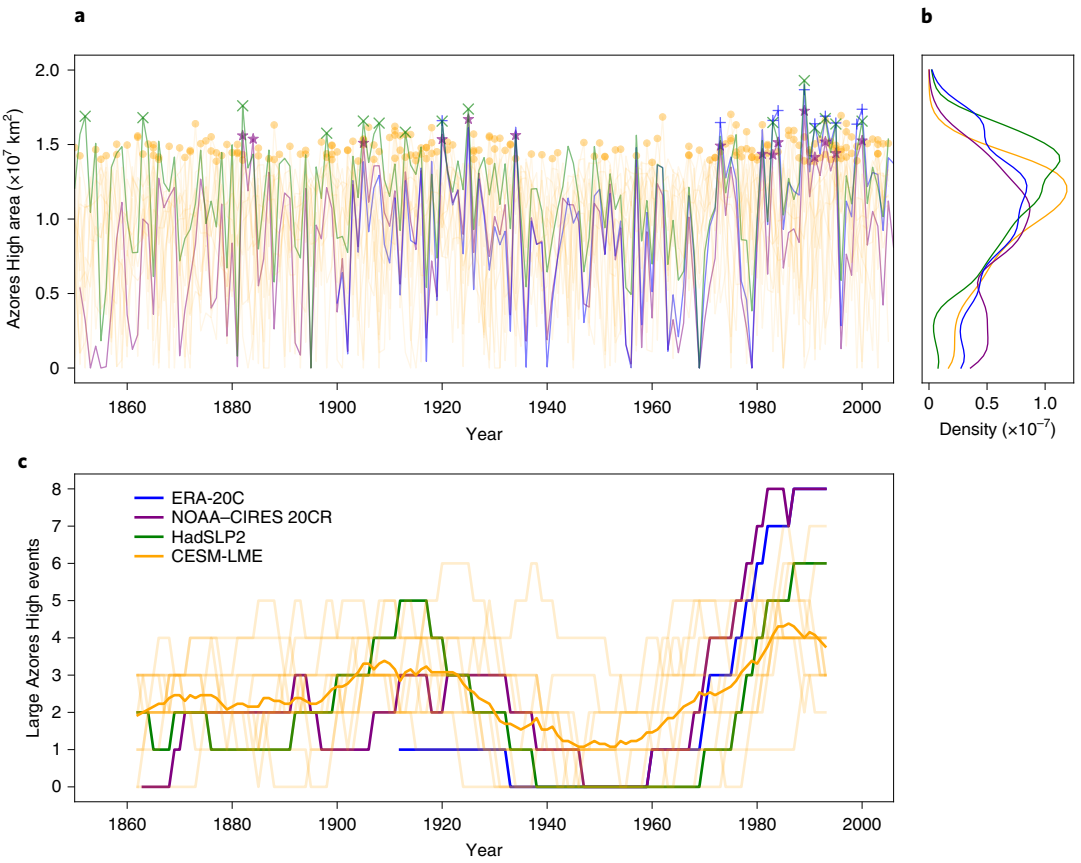

Fig. 2 | AHA in observations and simulations since 1850. a, Time series of AHA as reported by ERA-20C (blue), NOAA–CIRES 20CR (purple) and HadSLP2 (green) and as simulated by the 13 full-forcing members of the LME (light yellow). The winters with largest 10% of Azores High areas are indicated with crosses (ERA-20C), Xs (HadSLP2), stars (NOAA–CIRES 20CR) and circles (LME). **b**, Kernel density estimate for the AHA over the available period for reanalysis/observational data, as well as the kernel density estimate for the full-forcing members of the LME between 1850 and 2005. **c**, The number of winters with extremely large AHA that occur in a 25 yr window surrounding each year. The number of winters with extremely large AHA simulated by individual full-forcing members of the LME is shown in light yellow; the ensemble average is in bold yellow.

The frequency of winters with extreme AHA was determined for 25 yr periods surrounding each winter (Fig. 2c and Methods). Over the past 150 years, considerable multidecadal variability is visible in this frequency measure across the three observational and reanalysis products and well reproduced by the LME (Fig. 2c). The expansion of the Azores High measured as increasing frequency of extremely large events is clear in the late twentieth century and into the twenty-first century: in the most recent 25 yr period available (1980–2005), an average of 6.4 winters with extreme AHA occur across these data products; since 1850, the average number of extreme events per 25 yr period is 2.6 across datasets (Fig. 2c). While there is close agreement in the magnitude of the recent rapid rise in the number of winters with extreme AHA between the two reanalysis products (ECMWF Twentieth Century Reanalysis (ERA-20C) and NOAA–CIRES Twentieth Century Reanalysis (20CR)), Hadley Centre Sea Level Pressure dataset 2 (HadSLP2) reflects slightly less extreme AHA winters in the later part of the record. Finally, the LME displays a weaker expansion signal than the other three products in the late twentieth century. Notably, the LME's ensemble spread remains within the range of the observational and reanalysis products until 1980, when the reanalysis products record an even more dramatic Azores High expansion (Fig. 2c).

Despite the underestimated pace of the expansion in the LME since the 1980s, the level of agreement between the AHA in the LME and observational/reanalysis products throughout the past 150 years indicates that low-frequency variability in the Azores High is not merely internally driven but responds to common external forcing; that is, it can be simulated by climate models forced with realistic external forcings (Fig. 2). Furthermore, the coherence throughout the instrumental era suggests that the forcing prescribed in the LME's fully forced simulations[35] and the corresponding response of the LME accurately captures the multidecadal variability of the Azores High.

Unprecedented changes in the twentieth-century Azores High

To gauge whether the recent Azores High expansion is within the range experienced throughout past centuries, we analysed the full temporal extent offered by the LME simulations (CE 850 to CE 2005). We found that the industrial-era Azores High behaves differently from its pre-industrial counterpart. The industrial-era AHA distribution is skewed significantly larger than in pre-industrial times (Fig. 3b; $P<0.01$ according to the Kruskal–Wallis test by ranks). This difference is also visible in the frequency of extreme AHA events. The length of the LME simulations allows us to analyse the frequency of extreme events over longer, 100 yr, periods and explicitly capture the centennial variability. In the twentieth century, the LME averaged 15.2 winters with extremely large AHA; the average for all other 100 yr periods is 9.9 (Fig. 3a). The Monte Carlo sampling confirms that this difference in extreme event frequency is significant to $P<0.01$ (Fig. 3c). In 75% of LME simulations, the

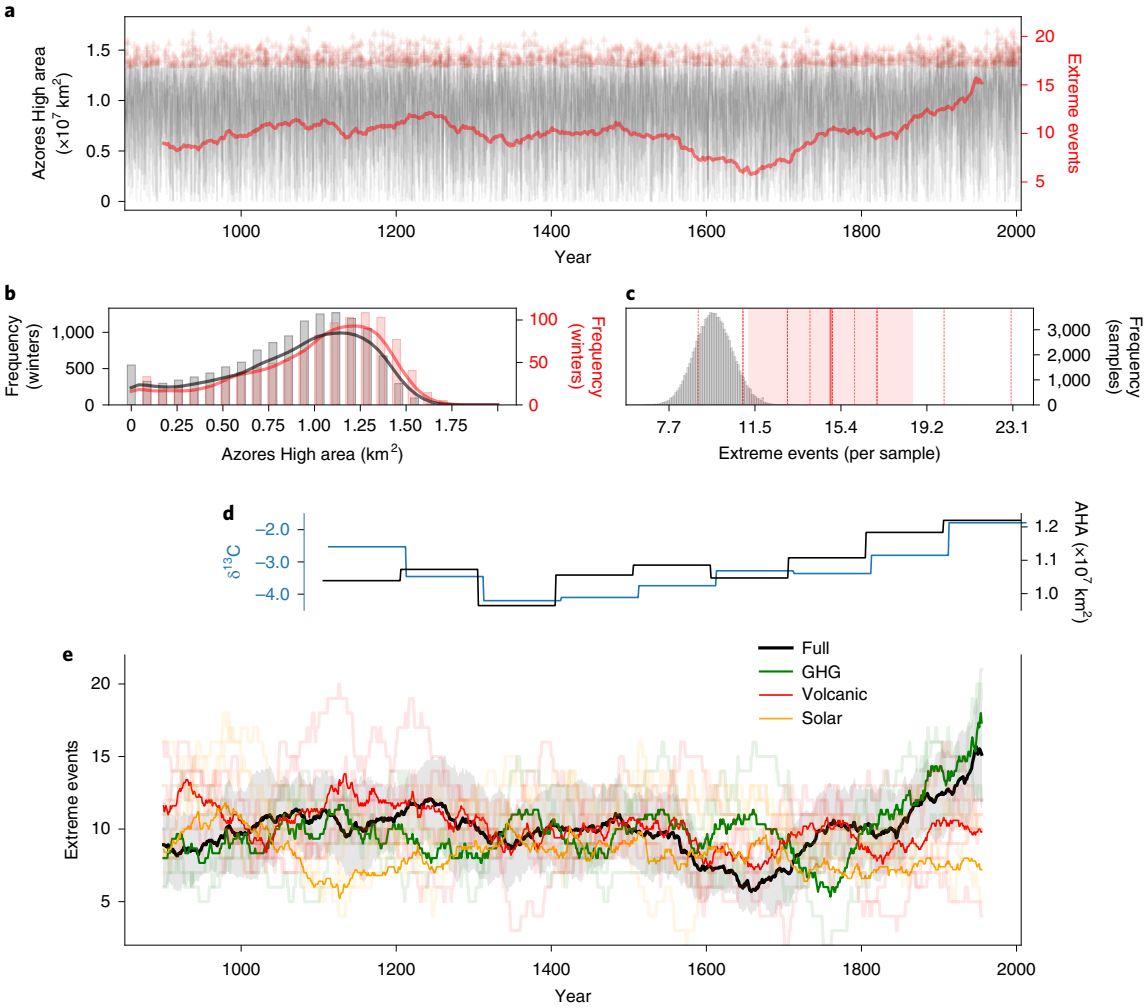

Fig. 3 | AHA and number of extreme events over the past millennium. a, Time series of AHA and number of winters with extremely large Azores Highs in a 100 yr window centred at each year for the ensemble mean (red line), individual ensemble members (grey lines) and individual extreme years (red triangles). **b**, Distributions of AHA during the industrial era (red) and the pre-industrial era (grey). **c**, Distribution of extremely large Azores High frequency (per 100 years) from Monte Carlo sampling from each ensemble member in grey. The red vertical lines show the number of extremely large Azores High events that occurred in the last 100 years of each ensemble member; their mean is in bold and ±1 s.d. is shaded. **d**, A 100 yr bin average comparison of AHA and a Suess effect-adjusted stalagmite carbon isotope record of hydroclimate from Buraca Gloriosa cave, Portugal[41]. The model and the isotope reconstruction show AHA size and related secular aridity in recent time to be unprecedented in the past 900 years. **e**, Ensemble mean frequency of winters with extremely large Azores Highs in a 100 yr window centred at each year for members with full forcing (black with grey shading for ±1 s.d.), GHGs only (green), volcanic (red) and solar (yellow); thick lines are ensemble mean; thin lines are individual forcing ensemble members.

most extreme 100 yr period has occurred within the past 200 years, indicating that the magnitude of recent changes is exceptional even in the context of internal climate variability. The low-frequency variability of the Azores High in the LME and the exceptionality of the past century are echoed by a regional hydroclimate proxy data sample from Portugal (Fig. 3d).

This industrial-era expansion is reproduced in several other Earth system models that simulate the past millennium (Extended Data Figs. 1 and 2). In addition to the CESM1.1 used to create the LME, we analysed five palaeoclimate models participating in the Paleoclimate Modelling Intercomparison Project phase 3 (PMIP3; Extended Data Table 2). As the PMIP3 Last Millennium experiments simulate the climate only from CE 850 to CE 1850, these experiments were combined with corresponding historical experiments to extend the modelled period to 2005. Using these combined experiments, we created a multimodel ensemble for comparison with the LME. We found that three other models (Beijing Climate Center Climate System Model 1.1 (BCC-CSM1.1), Community Climate System Model version 4 (CCSM4) and Max-Planck-Institut Earth System Model (MPI-ESM-P)) show a statistically significant increase in the AHA in the industrial era (Extended Data Fig. 1), while this is less pronounced in the other two models (Institut Pierre Simon Laplace Climate Model (IPSL-CM-LR), and Model for Interdisciplinary Research on Climate Earth System Model (MIROC-ESM); Extended Data Fig. 1). We also found that four of the five models had greater than average frequency of winters with extremely large AHA in the industrial era compared with pre-industrial (Extended Data Fig. 1). Furthermore, across all five PMIP3 models, the number of winters with extremely large Azores High has risen since 1900 (Extended Data Fig. 2). Selecting the last 100 years from each model's historical experiment, we found that the recent increase in extreme AHA frequency compared with other 100 yr periods throughout the past millennium is significant to $P < 0.02$ (Extended Data Fig. 2).

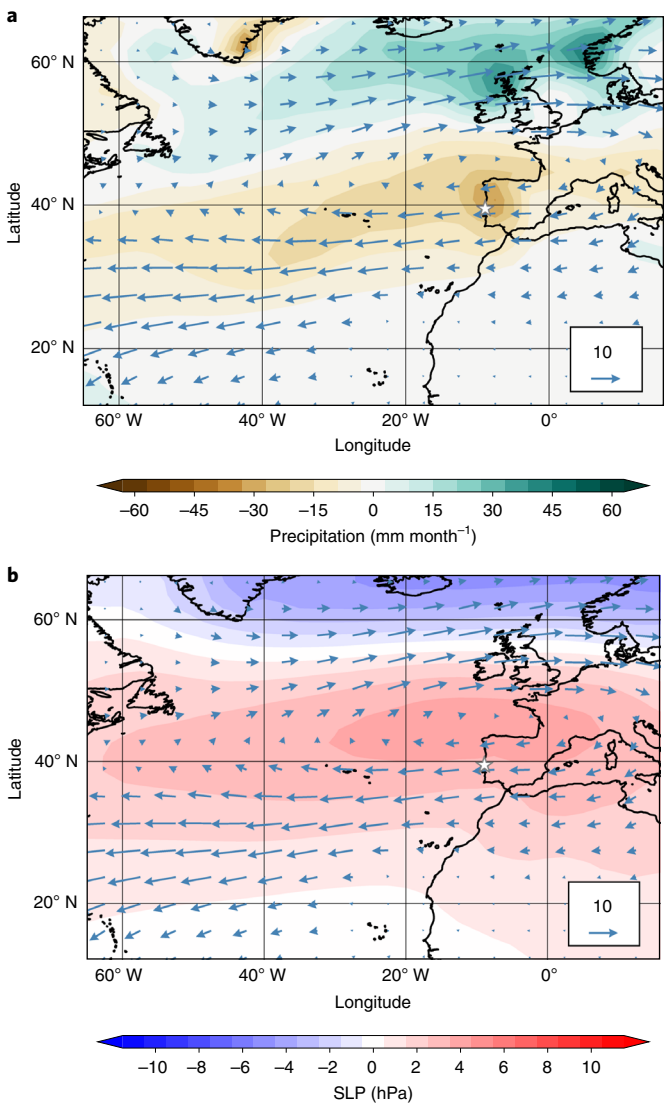

Fig. 4 | Hydroclimate during winters with extremely large Azores High. **a**, Anomalies of precipitation (contours) and moisture transport in $g\,kg^{-1}\,m\,s^{-1}$ (vectors) during winters with extremely large Azores High. Anomalies are calculated as the average difference between conditions during extremely large Azores High events and all other winter conditions. **b**, SLP (contours) and moisture transport anomalies during extremely large Azores High events. Anomaly patterns were calculated using the LME. The star above central Portugal indicates the location of Buraca Gloriosa cave.

Attribution of the unprecedented twentieth-century Azores High expansion

The coherence of Azores High expansion seen between the fully forced simulations within the LME (Fig. 3) suggests that Azores High expansion is not due to internal climate variability, but instead is driven by external forcings that are common to all simulations. For each of these external forcings, the LME includes a sub-ensemble (3–5 simulations) in which only one of the external forcings was varied. We performed an analysis of extreme AHA events within each of these sub-ensembles to explore the drivers of the change in Azores High behaviour. The only sub-ensemble members that show the expansion identified in the full-forcing simulations are the simulations in which GHG concentration is the only varied forcing (Fig. 3e). This indicates that the dramatic industrial-era expansion of the Azores High in a warming climate is a result of the anthropogenic increase in atmospheric GHG concentrations.

The increase in the number of winters with an extremely large Azores High in the industrial era is acutely felt on the Iberian Peninsula and in Northern Europe and the British Isles. Observations show that extremely large Azores High events bring on average 35.3 mm $month^{-1}$ (roughly 33% of the mean winter rainfall) less rainfall to the western coast of the Iberian Peninsula due to an anomalous reduction in onshore moisture transport (Fig. 4 and Extended Data Fig. 3). The spatial pattern of the drying brought about by extremely large Azores High events is consistent with changes in rainfall observed throughout the industrial era (Figs. 1a and 4 and Extended Data Fig. 3). Increasingly frequent extreme winters with an expanded Azores High have corresponded to the drying patterns seen in the industrial era. The significance of a winter with an extremely large Azores High to western Mediterranean hydroclimate is consistent across datasets and models (Extended Data Figs. 3 and 4).

Implications for climate risk

In this study, we have identified a robust increase in the frequency of extremely large AHA events and an overall expansion signal in the winter Azores High over the past 100 years. This expansion is consistent with a predominantly positive NAO in recent decades, which has been linked to decreased blocking in the eastern North Atlantic over the twentieth century[36], dry conditions over western Europe[27,37] and thinning of Arctic sea ice[38] and is shown to have teleconnections to temperature variability in the eastern Mediterranean[39]. An expanding Azores High agrees with reports of a poleward shift in the North Atlantic storm track and an increase in anticyclone frequency at the Azores High's poleward edge as well as a positive trend in regional subtropical indicators[15,26,40]. In addition, the Azores High expansion is consistent with a regional manifestation of an expanding Hadley Circulation. We have also linked the extremely large winter Azores High events during the past millennium to dry conditions on the Iberian Peninsula. This connection supports the correspondence between regional palaeohydroclimate and subtropical atmospheric variability on multidecadal to centennial time scales[41].

Previously, there has been a lack of consensus as to whether the trends seen in North Atlantic climate since 1980 are part of the system's natural variability or anthropogenically forced as surface anticyclones are known to have substantial interannual variability[15,26,34,42]. Although past trends have been shown to result from non-anthropogenic external forcing such as solar variability and volcanic aerosols[42,43], studies into twentieth-century Hadley Cell expansion have been unable to separate expansion signals in the northern hemisphere from natural climate variability[22]. Here, we establish that the Azores High expansion is driven by external climate forcings and show that the only external forcing that produces this signal in the industrial era is atmospheric GHG concentrations. Our findings have important implications for projected changes in western Mediterranean hydroclimate throughout the twenty-first century, with further warming probably reflected in changes in extreme Azores High characteristics as shown here throughout the past millennium, and concomitant future climate risks posed to productive agricultural sectors, such as viticulture and olive plantations, across the Iberian Peninsula[4–6].

Online content

Any methods, additional references, Nature Research reporting summaries, source data, extended data, supplementary information, acknowledgements, peer review information; details of author contributions and competing interests; and statements of data and code availability are available at https://doi.org/10.1038/s41561-022-00971-w.

Received: 20 November 2020; Accepted: 19 May 2022;
Published online: 04 July 2022

References

1. Hartmann, D. L. et al. (2013). Observations: Atmosphere and Surface. In *Climate Change 2013: The Physical Science Basis*. In Fifth Assessment Report of the Intergovernmental Panel on Climate Change. Cambridge University Press, Cambridge, United Kingdom and New York, NY, USA.
2. Giorgi, F. & Lionello, P. Climate change projections for the Mediterranean region. *Glob. Planet. Change* **63**, 90–104 (2008).
3. Bindi, M. & Olesen, J. E. The responses of agriculture in Europe to climate change. *Regional Environ. Change* **11**, 151–158 (2011).
4. Arenas-Castro, S., Gonçalves, J. F., Moreno, M. & Villar, R. Projected climate changes are expected to decrease the suitability and production of olive varieties in southern Spain. *Sci. Total Environ.* **709**, 136161 (2020).
5. Moriondo, M. et al. Projected shifts of wine regions in response to climate change. *Climatic Change* **119**, 825–839 (2013).
6. Ayuda, M.-I., Esteban, E., Martín-Retortillo, M. & Pinilla, V. The blue water footprint of the Spanish wine industry: 1930–2015. *Water* https://doi.org/10.3390/w12071872 (2020).
7. Webster, P. J. The elementary Hadley Circulation. In *The Hadley Circulation: Present, Past and Future* (eds Diaz, H. F. & Bradley, R. S.) 9–60 (Springer, 2004).
8. O'Gorman, P. A. & Muller, C. J. How closely do changes is surface and column water vapor follow Clausius–Clapeyron scaling in climate change simulations. *Environ. Res. Lett.* **5**, 025207 (2010).
9. D'Agostino, R. & Lionello, P. The atmospheric moisture budget in the Mediterranean: mechanisms for seasonal changes in the Last Glacial Maximum and future warming scenario. *Quat. Sci. Rev.* **241**, 106392 (2020).
10. Sousa, P. M. et al. North Atlantic integrated water vapor transport—from 850 to 2100 CE: impacts of western European rainfall. *J. Clim.* **33**, 263–279 (2020).
11. Moberg, A., Sonechkin, D. M., Holmgren, K., Datsenko, N. M. & Karlen, W. Highly variable Northern Hemisphere temperatures reconstructed from low- and high-resolution proxy data. *Nature* **433**, 610–613 (2005).
12. Li, W., Li, L., Ting, M. & Liu, Y. Intensification of Northern Hemisphere subtropical highs in a warming climate. *Nat. Geosci.* **5**, 830–834 (2012).
13. He, C. et al. Enhanced or weakened Western North Pacific Subtropical High under global warming? *Sci. Rep.* https://doi.org/10.1038/srep16771 (2015).
14. Raible, C. C., Ziv, B., Saaroni, H. & Wild, M. Winter synoptic-scale variability over the Mediterranean Basin under future climate conditions as simulated by the ECHAM5. *Clim. Dyn.* **35**, 473–488 (2010).
15. D'Agostino, R., Scambiati, A. L., Jungclaus, J. & Lionello, P. Poleward shift of northern subtropics in winter: time of emergence of zonal versus regional signals. *Geophys. Res. Lett.* **47**, e2020GL089325 (2020).
16. Waugh, D. W. et al. Revisiting the relationship among metrics of tropical expansion. *J. Clim.* **31**, 7565–7581 (2018).
17. Grise, K. M. et al. Recent tropical expansion: natural variability or forced response? *J. Clim.* **32**, 1551–1571 (2019).
18. Karnauskas, K. B. & Ummenhofer, C. C. On the dynamics of the Hadley circulation and subtropical drying. *Clim. Dyn.* **42**, 2259–2269 (2014).
19. Li, W. et al. Changes to the North Atlantic subtropical high and its role in the intensification of summer rainfall variability in the southeastern United States. *J. Clim.* https://doi.org/10.1175/2010JCLI3829.1 (2011).
20. Li, W. et al. Impacts of the North Atlantic subtropical high on interannual variation of summertime heat stress over the conterminous United States. *Clim. Dyn.* **53**, 3345–3359 (2019).
21. Ioannidou, L. & Yau, M. K. A climatology of the Northern Hemisphere winter anticyclones. *J. Geophys. Res. Atmospheres* **113**, D08119 (2008).
22. Woollings, T., Gregory, J. M., Pinto, J. G., Reyers, M. & Brayshaw, D. J. Response of the North Atlantic storm track to climate change shaped by ocean–atmosphere coupling. *Nat. Geosci.* **5**, 313–317 (2012).
23. Marshall, J., Johnson, H. & Goodmann, J. A study of the interaction of the North Atlantic oscillation with ocean circulation. *J. Clim.* **14**, 1399–1421 (2001).
24. Demény, A. et al. (2020). Holocene hydrological changes in Europe and the role of the North Atlantic ocean circulation from a speleothem perspective. *Quat. Int.* https://doi.org/10.1016/j.quaint.2020.10.061 (2020).
25. Zappa, G., Ceppi, P. & Shepherd, T. G. Time-evolving sea-surface warming patterns modulate the climate change response of subtropical precipitation over land. *Proc. Natl Acad. Sci. USA* https://doi.org/10.1073/pnas.1911015117 (2020).
26. Pepler, A., Dowdy, A. & Hope, P. A global climatology of surface anticyclones, their variability, associated drivers and long-term trends. *Clim. Dyn.* **52**, 5397–5412 (2019).
27. Hurrell, J. W. & Van Loon, H. Decadal variations in climate associated with the North Atlantic Oscillation. *Climatic Change* **36**, 301–326 (1997).
28. Trouet, V. et al. Persistent positive North Atlantic Oscillation mode dominated the medieval climate anomaly. *Science* **324**, 78–80 (2009).
29. Olsen, J., Anderson, N. J. & Knudsen, M. F. Variability of the North Atlantic Oscillation over the past 5,200 years. *Nat. Geosci.* **5**, 808–812 (2012).
30. Lehner, F., Raible, C. C. & Stocker, T. F. Testing the robustness of a precipitation proxy-based North Atlantic Oscillation reconstruction. *Quat. Sci. Rev.* **45**, 85–94 (2012).
31. Ortega, P. et al. A model-tested North Atlantic Oscillation reconstruction for the past millennium. *Nature* **523**, 71–74 (2015).
32. Cook, E. R. et al. A Euro-Mediterranean tree-ring reconstruction of the winter NAO index since 910 CE. *Clim. Dyn.* **53**, 1567–1580 (2019).
33. Hernández, A. et al. A 2,000-year Bayesian NAO reconstruction from the Iberian Peninsula. *Sci. Rep.* **10**, 14961 (2020).
34. Visbeck, M. H., Hurrell, J. W., Polvani, L. & Cullen, H. M. The North Atlantic Oscillation: past, present, and future. *Proc. Natl Acad. Sci. USA* **98**, 12876–12877 (2001).
35. Otto-Bliesner et al. Climate variability and change since 850 CE: an ensemble approach with the Community Earth System Model. *Bull. Am. Meteorol. Soc.* **97**, 735–754 (2015).
36. Davis, R. E., Hayden, B. P., Gay, D. A., Phillips, W. L. & Jones, G. V. The North Atlantic Subtropical Anticyclone. *J. Clim.* **10**, 728–744 (1997).
37. Vicente-Serrano, S. M. et al. The NAO impact on droughts in the Mediterranean region. *Adv. Glob. Change Res.* **46**, 23–40 (2011).
38. Tucker, W. B., Weatherly, J. W., Eppler, D. T., Farmer, L. D. & Bentley, D. L. Evidence for rapid thinning of sea ice in the western Arctic Ocean at the end of the 1980s Greenland. *Geophys. Res. Lett.* **28**, 2851–2854 (2001).
39. Ben-Gai, T., Bitan, A., Manes, A., Alpert, P. & Kushnir, Y. Temperature and surface pressure anomalies in Israel and the North Atlantic Oscillation. *Theor. Appl. Climatol.* **69**, 171–177 (2001).
40. Yin, J. H. A consistent poleward shift of the storm tracks in simulations of 21st century climate. *Geophys. Res. Lett.* **32**, L18701 (2005).
41. Thatcher, D. L. et al. Hydroclimate variability from western Iberia (Portugal) during the Holocene: insights from a composite stalagmite isotope record. *Holocene* **30**, 966–981 (2020).
42. Alfaro-Sánchez, R. et al. Climatic and volcanic forcing of tropical belt northern boundary over the past 800 years. *Nat. Geosci.* **11**, 933–938 (2018).
43. Ait Brahim, Y. et al. Multi-decadal to centennial hydro-climate variability and linkage to solar forcing in the Western Mediterranean during the last 1000 years. *Sci. Rep.* **8**, 17446 (2018).

Publisher's note Springer Nature remains neutral with regard to jurisdictional claims in published maps and institutional affiliations.

© The Author(s), under exclusive licence to Springer Nature Limited 2022

Methods

Observational and reanalysis products. For observational SLP data, we use HadSLP2, created using spatially interpolated SLP observations[44] (Extended Data Table 1). It is important to note when working with extended observationally derived records that changes in the amount and quality of observations over time can introduce artefacts. For this reason, we use several different data products, including reanalysis, to analyse SLP. For observations of terrestrial rainfall, we use the Global Precipitation Climatology Centre's (GPCC's) monthly data V7, which offers quality-controlled gauge-based observations from over 67,000 stations worldwide[45]. Reanalysis, or retrospective analysis, combines assimilated observed variables with climate model simulations to create gridded climate data[46,47]. These products, when forced with the relatively accurate and extended record of surface pressure, become a powerful tool for studying climate[48]. We use NOAA–CIRES Twentieth Century Reanalysis ensemble means[46] and ERA-20C reanalysis products[47] for SLP and moisture transport. Moisture transport is calculated as the product of humidity at 850 hPa and the wind velocity at 850 hPa. Both observational and reanalysis data offer global gridded coverage, which allowed us to perform analysis that is replicable with climate model output. Each dataset covers the entire twentieth century, which allows a long-term comparison with the simulations offered by the LME (for more information, see Extended Data Table 1).

LME. The LME is an ensemble of numerical simulations that model the climate of the past millennium using CESM1.1. The CESM1.1 is configured with ~2° and ~1° atmospheric and ocean horizontal resolution, respectively[49]. We note that CESM1.1 has been shown to not fully capture the southern extent of the eddy-driven jet in CESM Large Ensemble simulations[50]. To validate CESM1.1's representation of the Azores High, it has been compared with reanalysis/observation data over the instrumental era (Fig. 2) and found to skilfully capture multidecadal variability in the Azores High.

All simulations within the LME are branched off year 850 of a long-run spin-up and continue for 1,156 years until 2006[31]. All ensemble members start from year CE 850 of the 850-control run with random rounding applied to the initial temperature field. The ensemble contains 13 full-forcing simulations that receive identical transient volcanic, ozone/aerosols, solar variability, orbital variability and well-mixed atmospheric GHG forcings. From CE 850 to CE 1850, the transient forcings are identical to those used in phase 3 of the PMIP3 and the CCSM4 Last Millennium simulations[51]. The transient forcings from 1850 to 2006 are the same as those used in the historical simulations of the Coupled Model Intercomparison Project phase 5. The ensemble also includes simulations in which one of the transient external forcings is applied while the remaining external forcings are fixed at CE 850 levels. For these individual forcing simulations there are five volcanic only, three GHG only, four solar only, three orbital only and three land-use and land-change only. Each member of these smaller ensembles differs from each other by random rounding of the initial temperature field.

PMIP3 models. As validation of the CESM1.1 model, we analysed five palaeoclimate models participating in the PMIP3 (Extended Data Table 2)[52–57]. As PMIP3 Last Millennium experiments simulate the climate only from CE 850 to CE 1850, we combined these experiments with corresponding historical experiments to extend the modelled period to 2005. Historical simulations are initialized at 1850 with a pre-industrial control run, and so this does not offer a continuous simulation from CE 850 to 2005 as the LME does[58]. By combining the experiments, however, we have five different modelled records of pre-industrial and industrial climate, each simulated by a different numerical climate model. The historical and last millennium simulations used the same modelling components, structure and resolution for each of the models used. Using these combined experiments, we created a multimodel ensemble (MME). For comparison with the LME, we found the frequency of winters since CE 850 with an extremely large Azores High with this MME (Extreme event analyses). We also compared the frequency of extreme events in the past 100 years with previous centuries to ensure that the results found in the LME are produced by other models as well (Monte Carlo validation; results in Azores High expansion in PMIP3). Note that models within this MME have been shown to represent the North Atlantic storm track as being overly zonal and elongated[59,60]. Despite these deficiencies, it is important to compare results found in the LME with other models of the Earth system.

AHA. To quantify the variability of the Azores High, we use an AHA diagnostic. The AHA was defined as the area (km^2) over the North Atlantic and Western Europe that had mean winter (December–January–February) SLP greater than 0.5 s.d. from the mean of the spatio-temporal winter SLP distribution (Fig. 1b). The region considered when calculating the AHA is bounded by the 60° W and 10° E meridians as well as the 10° N and 52° N latitudes. This region includes much of the North Atlantic and Western Europe. The inclusion of Western Europe in this region allows the diagnostic to capture the tendency of the Azores High to encroach onto continental Europe during the winter months. By creating a relative high-pressure threshold based on statistical features of the North Atlantic region, we accommodate differences in variance across datasets. To maintain the dynamical relevance of the AHA metric in a changing climate with a transient mean state, we have removed the global SLP linear trend since 1850 before calculating the AHA. The result is a simple diagnostic that captures variability in the size of the Azores High and tracks the dynamical response to this variability (Fig. 4 and Extended Data Figs. 3 and 4).

Extreme event analyses. To track the frequency of winters with extreme AHA in a multi-simulation ensemble, such as the LME or MME, we employed a running bin analysis. To perform this analysis, we first calculated a time series of AHA (AHA). Second, we identified winters in which the Azores High was extremely large (within the largest 10% of winter Azores Highs; 'non-extreme' winters or events refers to winters that have not met this criterion). Finally, we recorded the frequency of these extremely large Azores High events in the 100 yr period surrounding each winter. This analysis created a frequency record of extremely large Azores High events, which corresponds to drought conditions on the Iberian Peninsula (Fig. 4), that can be compared between ensemble members. In this way, the running bin analysis provided a vital tool for inter-ensemble comparison and attribution of external climate drivers. When applying running bin analysis to shorter time series, such as those of observational records, we assessed only the 25 years surrounding each year. When applying the running bin analysis to the PMIP3 model output, we analysed 100 yr periods throughout the Last Millennium and Historical experiments.

Note that this diagnostic is not targeted at identifying individual synoptic events, as are associated with individual atmospheric blocking events. For example, the diagnostic is agnostic whether a particular winter was identified as extreme because the Azores High was extremely large throughout the winter or through an accumulation of individual synoptic events that periodically resulted in larger areal extent of the Azores High; the latter would have required daily climate model output that would have severely limited data availability. From previous work[61] on atmospheric blocking across the North Atlantic sector in reanalysis products, it appears that monthly data can be used to skilfully represent year-to-year variability in winter atmospheric blocking across the region.

Monte Carlo validation. The analysis of the AHA in the LME shows that, across ensemble members, the twentieth century featured a high frequency of extremely large Azores High winters (see Unprecedented changes in the twentieth-century Azores High). To test the significance of the increase in frequency of extremely large Azores High winters, we utilised Monte Carlo sampling. The aim was to calculate the probability that randomly selecting a 100 yr period from each ensemble member would produce the same frequency of extremely large Azores High winters as was simulated for the twentieth century. For each Monte Carlo sample, we randomly selected a 100 yr period from each ensemble member of the LME and totalled the number of extremely large Azores High events occurring in these 100 yr periods. We took 100,000 such samples, creating a normal distribution. We then selected the last 100 years of each ensemble member and totalled the number of extremely large Azores High winters. This was compared with the distribution created using Monte Carlo sampling to find the probability that the last 100 years of the ensemble experienced the high frequency of extremely large Azores High events by chance. The same Monte Carlo sampling was invoked to test the significance of the high frequency of extremely large Azores High winters in the MME as well.

Isotope reconstruction. To validate the long-term variability and behaviour of the Azores High in the LME, we compared it with hydroclimate proxy data from the region, namely, a multi-proxy composite record from six well-dated and overlapping speleothems from Buraca Gloriosa cave located in western Portugal, which is in the heart of the region affected by Azores High variability[41] (Fig. 1). The Buraca Gloriosa composite record was generated from stalagmite stable isotope data and U–Th ages[41] and was corrected for the Suess effect following the methods of Verburg[62] and Railsback[63] and combined into 100 yr bins.

Azores High expansion in PMIP3. The results from this study leverage the robustness of the LME as a tool for diagnosing and attributing changes in climate. The LME was assembled using the CESM1.1 model, which has been shown to agree with climate reconstructions of the past millennium[31]. To further validate the LME and the CESM1.1 model specifically, we analysed experiments from other models that simulate this period (PMIP3 models). We found that other models (BCC-CSM1.1, CCSM4 and MPI-ESM-P) show a visible and statistically significant increase in average AHA in the industrial era (Extended Data Fig. 1b,d,j). This difference is less pronounced in two further models analysed in this study (IPSL-CM5A-LR and MIROC-ESM; Extended Data Fig. 1f,h). We also found that all models, except MIROC-ESM, had greater than average extremely large Azores High event frequency in the industrial era (Extended Data Fig. 1a,c,e,g,i). Because of individual biases in SLP and difference in atmospheric resolution, an MME mean comparison of the AHA is not appropriate. Unlike the size of the Azores High, the frequency of extremely large Azores High events is a relative statistic and can be averaged across models to perform robust ensemble analysis. This analysis showed that across models, the event frequency of winters with extremely large Azores High increased significantly in the industrial era (Extended Data Fig. 2a). To determine significance, we used Monte Carlo sampling (Monte Carlo validation) to select 100 years from each model, total the extreme events and

form a distribution (Extended Data Fig. 2b). Selecting the last 100 years from each model's historical experiment, we found the increase in extreme event frequency is significant to $P=0.02$. This is a lower significance threshold than the results from the Monte Carlo validation on the LME. This is perhaps due to the smaller size of the ensemble (5 members instead of 13).

Extremely large Azores High events. In the LME simulations, we found a significant and intuitive connection between the size of the Azores High and hydroclimate in Europe (Fig. 4). To ensure that the AHA was representing the same dynamics, and particularly that the extremely large Azores High winters were comparable across datasets, we found the precipitation, moisture transport and SLP anomalies during extremely large Azores High events in reanalysis/observations (Extended Data Fig. 3) and other model simulations (Extended Data Fig. 4). For the observational/reanalysis composites (Extended Data Fig. 3a–d), the occurrence of extremely large Azores High events and the moisture transport anomalies we calculated with reanalysis products (ERA-20C and NOAA–CIRES-20CR) and the precipitation anomalies during these extreme Azores High events were calculated with observational precipitation data (GPCC V7). All composites (Extended Data Figs. 3 and 4) show similar precipitation and moisture transport anomalies associated with an extremely large Azores High, showing that these events are closely tied with the hydroclimate of Europe.

Testing significance. To test the significance of the expanding Azores High, we employed two different methods. The first method was a Kruskal–Wallis *H* test. This method was chosen to assess the possibility that the industrial-era AHA has the same median as the pre-industrial AHA. The Kruskal–Wallis *H* test allows for non-parametric distributions. This is necessary because both the pre-industrial and industrial AHA distributions are skewed left. The shape and scale of the industrial and pre-industrial AHA distributions are similar (Fig. 3b). As the Kruskal–Wallis test result passes our significance threshold $P<0.01$, we can reject the hypothesis that the medians of the two distributions are equal, indicating two significantly different distributions.

We wanted to test the likelihood that sampling extreme events from the last 100 years of each simulation was the same as sampling throughout the entire length of the simulations. To do this, we formed a distribution of total extremely large Azores High events in 13 randomly selected 100 yr periods (a 100 yr period from each simulation). We compared the number of extreme events in the last 100 years of each simulation with this distribution. We found the probability of randomly selecting a sample with at least as many extreme events as the last 100 years of each simulation to be less than 0.01%.

Data availability

Observational datasets are publicly accessible at NOAA/OAR/ESRL PSL, Boulder, Colorado, USA, from their website at https://psl.noaa.gov/; and ERA-20C from ECMWF (https://www.ecmwf.int/en/forecasts/datasets/reanalysis-datasets/era-20c). Climate model output is publicly available as follows: CESM LME (https://www.cesm.ucar.edu/projects/community-projects/LME/) is available through Earth System Grid (https://www.earthsystemgrid.org/dataset/ucar.cgd.ccsm4.cesmLME.html), PMIP3 data through https://esgf-node.llnl.gov/search/cmip5/. Stable isotope data in Fig. 3d are available through NCEI at https://www.ncei.noaa.gov/access/paleo-search/study/29392.

Code availability

Code used to perform the analysis presented in this study is provided as part of the replication package. It is available at https://github.com/nathanielcresswellclay/AzoresHighExpansion.

References

44. Allan, R. & Ansell, T. A new globally complete monthly historical gridded mean sea level pressure dataset (HadSLP2): 1850-–2004. *J. Clim.* **19**, 5816–5842 (2006).
45. Schneider, U. et al. *GPCC Full Data Reanalysis Version 6.0 at 0.5°: Monthly Land-Surface Precipitation from Rain-Gauges Built on GTS-Based and Historic Data* (GPCC, 2011); https://doi.org/10.5676/DWD_GPCC/FD_M_V7_050
46. Compo, G. P. et al. The twentieth century reanalysis project. *Q. J. R. Meteorol. Soc.* **137**, 1–28 (2011).
47. Poli, P. et al. ERA-20C: an atmospheric reanalysis of the twentieth century. *J. Clim.* **29**, 4083–4097 (2016).
48. Compo, G. P., Whitaker, J. S. & Sardeshmukh, P. D. Feasibility of a 100-year reanalysis using only surface pressure data. *Bull. Am. Meteorol. Soc.* **87**, 175–190 (2006).
49. Hurrell, J. W. et al. The Community Earth System Model: a framework for collaborative research. *Bull. Am. Meteorol. Soc.* **94**, 1339–1360 (2013).
50. Kwon, Y. O. et al. North Atlantic winter eddy-driven jet and atmospheric blocking variability in the Community Earth System Model version 1 Large Ensemble simulations. *Clim. Dyn.* **51**, 3275–3289 (2018).
51. Landrum, L. et al. Last millennium climate and its variability in CCSM4. *J. Clim.* **26**, 1085–1111 (2013).
52. Xin, X. G., Wu, T. W. & Zhang, J. Introduction of CMIP5 experiments carried out with the climate system models of Beijing climate center. *Adv. Clim. Change Res.* **4**, 41–49 (2013).
53. Gent, P. R. et al. The Community Climate System Model version 4. *J. Clim.* **24**, 4973–4991 (2011).
54. Dufresne, J. L. et al. Climate change projections using the IPSL-CM5 Earth system model: from CMIP3 to CMIP5. *Clim. Dyn.* **40**, 2123–2165 (2013).
55. Sueyoshi, T. et al. Set-up of the PMIP3 paleoclimate experiments conducted using an Earth system model, MIROC-ESM. *Geosci. Model Dev.* **6**, 819–836 (2013).
56. Watanabe, S. et al. MIROC-ESM 2010: model description and basic results of CMIP5-20c3m experiments. *Geosci. Model Dev.* **4**, 845–872 (2011).
57. Giorgetta, M. A. et al. Climate and carbon cycle changes from 1850 to 2100 in MPI-ESM simulations for the Coupled Model Intercomparison Project phase 5. *J. Adv. Model. Earth Syst.* https://doi.org/10.1002/jame.20038 (2013).
58. Taylor, K. E., Stouffer, R. J. & Meehl, G. A. An overview of CMIP5 and the experiment design. *Bull. Am. Meteorol. Soc.* **93**, 485–498 (2012).
59. Zappa, G., Shaffrey, L. & Hodges, K. The ability of CMIP5 models to simulate North Atlantic extratropical cyclones. *J. Clim.* **26**, 5379–5396 (2013).
60. Colle, B. A. et al. Historical evaluation and future prediction of eastern North American and Western Atlantic extratropical cyclones in the CMIP5 models during the cool season. *J. Clim.* **26**, 6882–6903 (2013).
61. Kwon, Y. O., Seo, H., Ummenhofer, C. C. & Joyce, T. M. Impact of multidecadal variability in Atlantic SST on winter atmospheric blocking. *J. Clim.* **33**, 867–892 (2020).
62. Verburg, P. The need to correct for the Suess effect in the application of $\delta^{13}C$ in sediment of autotrophic Lake Tanganyika, as a productivity proxy in the Anthropocene. *J. Paleolimnol.* **37**, 591–602 (2007).
63. Railsback, L. B. et al. A multi-proxy climate record from a northwestern Botswana stalagmite suggesting wetness late in the Little Ice Age (1810–1820 CE) and drying thereafter in response to changing migration of the tropical rain belt or ITCZ. *Palaeogeogr. Palaeoclimatol. Palaeoecol.* **506**, 139–153 (2018).

Acknowledgements

Use of the following datasets is gratefully acknowledged: Global Precipitation Climatology Center dataset by the German Weather Service (DWD), HadSLP2 from the UK Hadley Centre and NOAA–CIRES Twentieth Century Reanalysis, all provided by the NOAA/OAR/ESRL PSL, Boulder, Colorado, USA, from their website at https://psl.noaa.gov/; ERA-20C from ECMWF. Support for the Twentieth Century Reanalysis Project version 2c dataset is provided by the US Department of Energy, Office of Science Biological and Environmental Research (BER) and by the National Oceanic and Atmospheric Administration Climate Program Office. We acknowledge the CESM1(CAM5) Last Millennium Ensemble Community Project and supercomputing resources provided by NSF/CISL/Yellowstone, as well as the World Climate Research Programme's Working Group on Coupled Modelling, which is responsible for CMIP, and we thank the climate modelling groups for producing and making available their model output, with specific contributions from Beijing Climate Center's Climate System Modelling Division, the National Center for Atmospheric Research, Institut Pierre Simon Laplace's Climate Modelling Center, Max-Planck-Institut fur Meteorologie's Modelling Division and the Atmosphere and Ocean Research Institute at the University of Tokyo. CMIP5 model output was provided by the WHOI CMIP5 Community Storage Server via their website: http://cmip5.whoi.edu/. Cave research at Buraca Gloriosa conducted with the assistance of Associação de Estudos Subterrâneos e Defesa do Ambiente and Jonathan Haws. This work was supported by the US National Science Foundation (grants: AGS-1804528 to A.D.W.; AGS-1804635 to R.F.D.; AGS-1804132 to C.C.U.), Cornell College (to R.F.D.) and the Ocean Climate Change Institute and James E. and Barbara V. Moltz Fellowship for Climate-Related Research at WHOI (to C.C.U.).

Author contributions

N.C.-C. and C.C.U. conceived the study and designed the analyses. N.C.-C. conducted all the analyses. N.C.-C. and C.C.U. wrote the manuscript. D.L.T., A.D.W. and R.F.D. provided feedback on the analyses and manuscript. Y.A. and V.J.P. provided feedback on the manuscript.

Competing interests

The authors declare no competing interests.

Additional information

Extended data is available for this paper at https://doi.org/10.1038/s41561-022-00971-w.

Correspondence and requests for materials should be addressed to Caroline C. Ummenhofer.

Peer review information *Nature Geoscience* thanks Pedro Sousa and the other, anonymous, reviewer(s) for their contribution to the peer review of this work. Primary Handling Editor: James Super, in collaboration with the *Nature Geoscience* team.

Reprints and permissions information is available at www.nature.com/reprints.

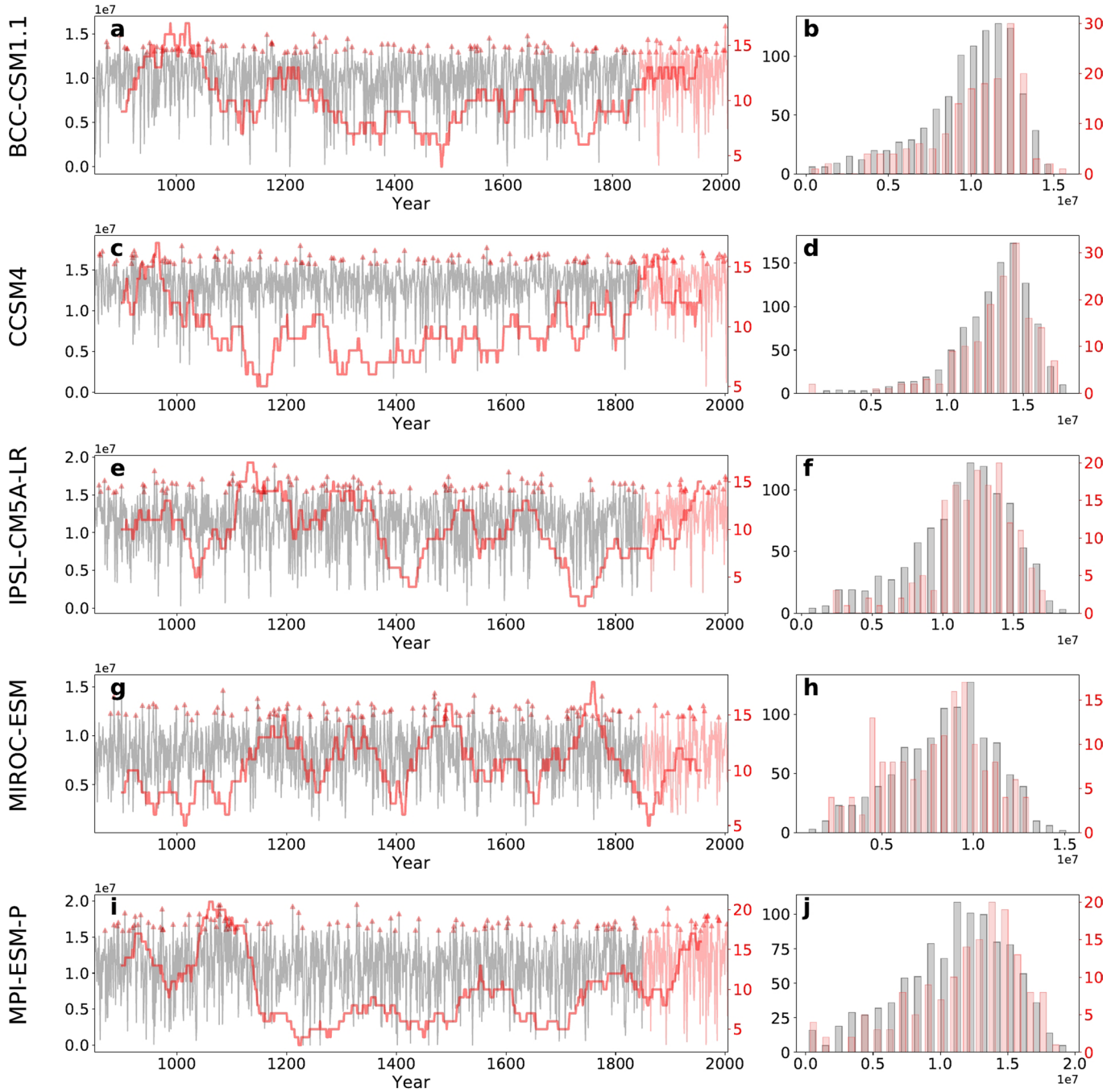

Extended Data Fig. 1 | Azores High Area in PMIP3 Models. (a,c,e,g,i) Timeseries of Azores High Area (AHA) during the PMIP3 last millennium (grey) and historical (light red) simulations. Extremely large events are indicated as red triangles. Thick red line represents the number of extreme winters in the 100-year period surrounding each year. (b,d,f,h,j) Distribution of AHA during the last millennium (grey) and historical (red) simulations. Each row is calculated using output from the model indicated on the left. For more information on models see Methods: PMIP3 Models.

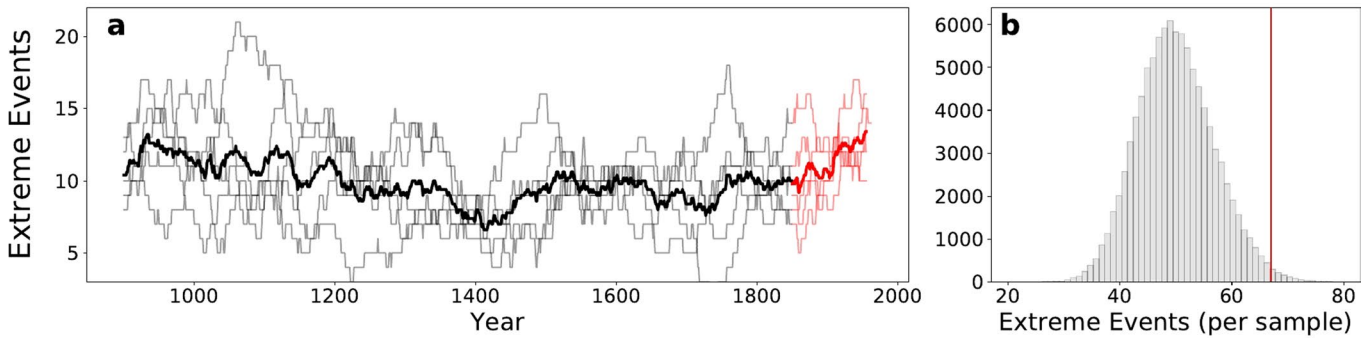

Extended Data Fig. 2 | Extremely Large Azores High Area in PMIP3 Models. (a) The number of winters with extremely large Azores High in the 100-year period surrounding each year for PMIP3 last millennium (grey) and historical (red) simulations. The Multi Model Ensemble average is shown for the last millennium (thick black) and historical (thick red) simulations. (b) The results of our Monte Carlo test for significance of extremely large Azores High winters (see Methods: Monte Carlo Validation) for the Multi Model Ensemble. The red vertical line shows the number of extremely large Azores High winters that occurred in the last 100 years of the historical simulation; this is significant to $p = 0.02$ (see Methods: Monte Carlo Validation). The models and simulations used are discussed in Methods: PMIP3 Models.

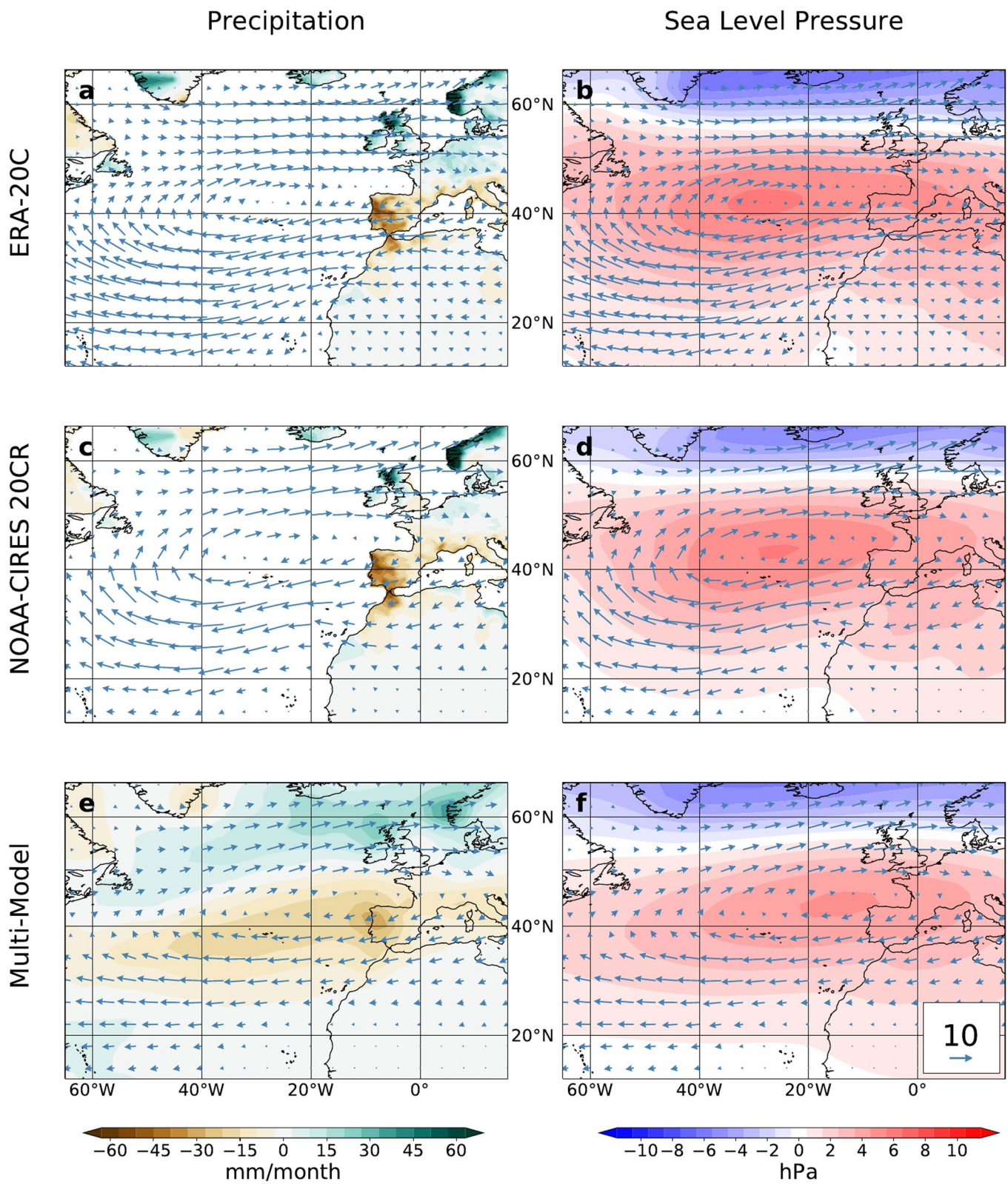

Extended Data Fig. 3 | Hydroclimate during winters with extremely large Azores High in observations and models. (a,c,e) Wintertime anomalies in precipitation (contours) and moisture transport in g kg^{-1} m s^{-1} (vectors) during winters with extremely large Azores High. (b,d,f) Wintertime anomalies in sea level pressure (contours) and moisture transport (vectors) during winters with extremely large Azores High. Each row was calculated using the dataset indicated to the left. Precipitation in (a) and (c) is based on the GPCC dataset. The multi-model ensemble was calculated using PMIP3 models interpolated onto a regular 2° by 2°grid.

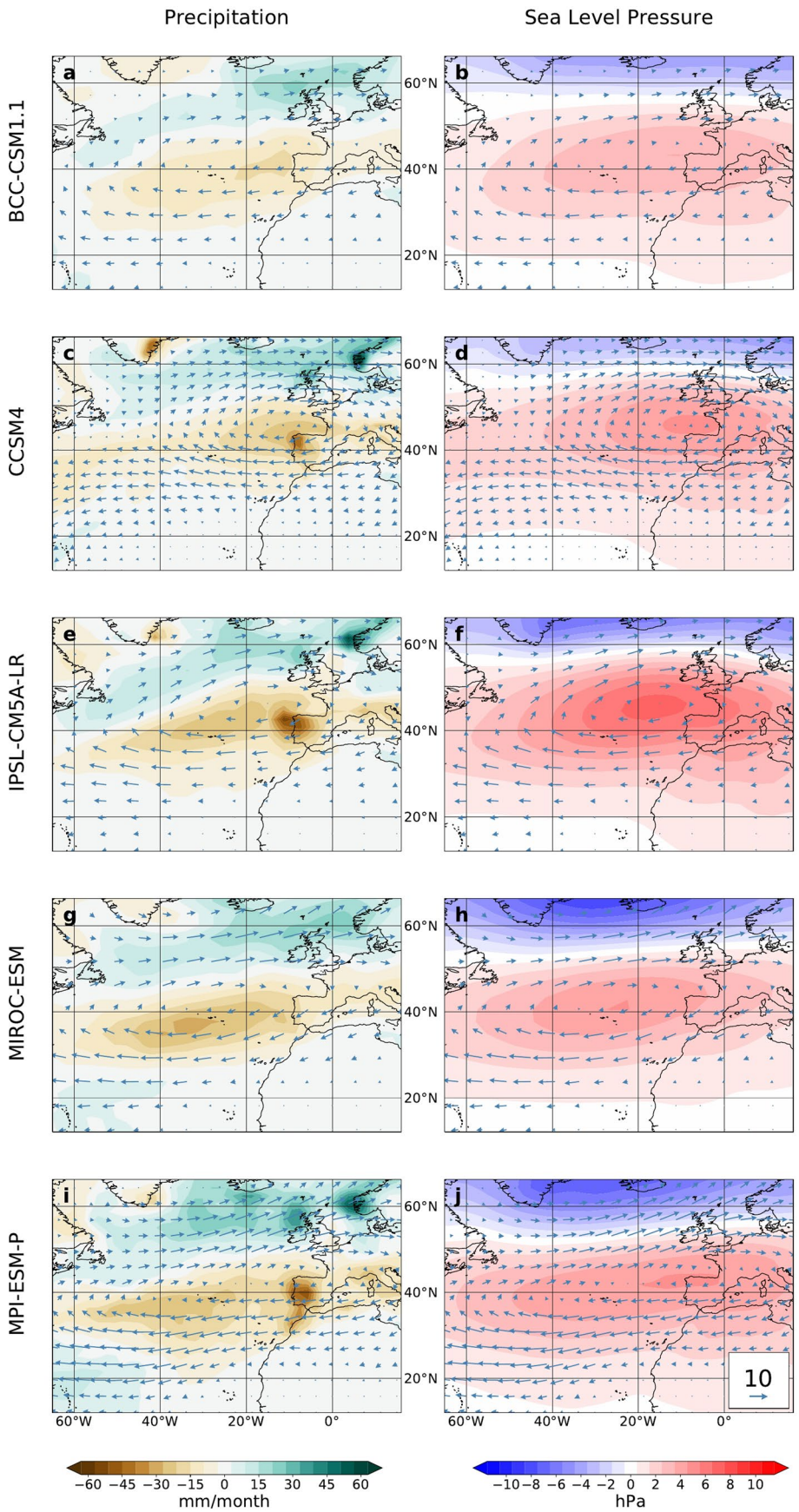

Extended Data Fig. 4 | See next page for caption.

Extended Data Fig. 4 | Hydroclimate during winters with extremely large Azores High in individual models. (a,c,e,g,i) Wintertime anomalies in precipitation (contours) and moisture transport in g kg^{-1} m s^{-1}(vectors) during winters with extremely large Azores High. (b,d,f,h,j) Anomalies in sea level pressure (contours) and moisture transport (vectors) during winters with extremely large Azores High. Each row was calculated using output from the models indicated to the left. For information on models and simulations see Extended Data Table 2.

Extended Data Table 1 | Summary of the observational and reanalysis products used in the study

Acronym	Institute	Start date	Dataset Type	Resolution	Reference
HadSLP2	Met Office Hadley Centre for Climate Science and Services, UK	1850	Observational	5° latitude by 5° longitude	Allan and Ansell 2006[44]
NOAA-CIRES-20CR	National Oceanic and Atmospheric Administration, USA	1851	Reanalysis	2° latitude by 2° longitude	Compo et al. 2011[46]
ERA 20C	European Centre for Medium-Range Weather Forecasts	1900	Reanalysis	1° latitude by 1° longitude	Poli et al. 2016[47]
GPCC	Global Precipitation Climatology Centre	1901	Observational	0.5° latitude by 0.5° longitude	Schneider et al. 2011[45]

Sources, time range and resolution are provided. For technical information on each dataset see listed reference documents for the products.

Extended Data Table 2 | Summary of the Paleo Model Intercomparison Project phase 3 (PMIP3) models and experiments used in the study

Model	Institute	Resolution	Experiments	Ensemble	Acronym	References
BCC-CSM1.1	BCC, China	2.8° latitude by 2.8° longitude	Last Millennium, Historical	r1i1p1	BCC	Xin et al. 2013[58]
CCSM4	NCAR, USA	0.94° latitude by 1.25° longitude	Last Millennium, Historical	r1i1p1	CCSM	Gent et al. 2011[59]
IPSL-CM5A-LR	IPSL, France	1.89° latitude by 3.75° longitude	Last Millennium, Historical	r1i1p1	IPSL	Dufresne et al. 2013[60]
MIROC-ESM	MIROC, Japan	2.8° latitude by 2.8° longitude	Last Millennium, Historical	r1i1p1	MIROC	Sueyoshi et al. 2013[61], Wantanabe et al. 2011[62]
MPI-ESM-P	MPI-M, Germany	1.86° latitude by 1.88° longitude	Last Millennium, Historical	r1i1p1	MPI	Giorgetta et al. 2013[63]

The atmospheric component resolutions are given. The models and their respective institutions are indicated. For more technical information on the model structure and contribution to PMIP3 refer to the associated reference. See Methods: PMIP3 models for discussion of simulations and model specifics.